

Temperature dependence of the thermal expansion of GaN

C. Roder,* S. Einfeldt, S. Figge, and D. Hommel

Institute of Solid State Physics, University of Bremen, P.O. Box 330 440, 28334 Bremen, Germany

(Received 8 July 2005; published 24 August 2005)

The thermal expansion of hexagonal GaN bulk crystals was studied in an extended temperature range from 12 to 1025 K. The lattice parameters a and c were measured by high-resolution x-ray diffraction. The temperature dependence of the derived thermal expansion coefficients along the a and c directions could be well described over the entire temperature range within both the Debye model and the Einstein model. Debye temperatures of (868 ± 20) K and (898 ± 24) K and Einstein temperatures of (636 ± 13) K and (662 ± 18) K were derived along the a and c axes, respectively, and compared to available literature values.

DOI: [10.1103/PhysRevB.72.085218](https://doi.org/10.1103/PhysRevB.72.085218)

PACS number(s): 65.40.De, 61.10.Nz, 81.05.Ea

I. INTRODUCTION

Thermal expansion is one of the very fundamental properties of a crystalline solid. It results from the anharmonicity of the interatomic potential and can be related to the intrinsic energy of the solid similar to the specific heat and the thermal conductivity. In the case of epitaxial layers grown on foreign substrates the difference in the thermal expansion coefficients between the layer material and the substrate material governs the strain induced in the layer during cool down from growth to room temperature. This is of particular importance for GaN layers, which recently have attracted considerable interest due to their use for short-wavelength light emitting devices and high-power electronics. At present GaN is typically grown on substrates such as sapphire, SiC, or silicon because of the lack of commercially available GaN substrates. Both high compressive and tensile stresses have been reported for GaN layers. Because the strain determines various important parameters of GaN such as its bandgap energy, its internal electric field, and the onset of plastic deformation of its lattice, the accurate knowledge of the thermal expansion is essential not only from a physical point of view but also for device engineering.

The thermal expansion coefficients (TECs) along the a and c axis of GaN (α_a and α_c) have been studied experimentally during the past years using different types of samples such as GaN powder,¹⁻⁴ epitaxial layers,⁵⁻¹⁰ and bulk crystals,^{6-8,10} and covering different temperature ranges. However, the available data scatter significantly such that more precise measurements are needed. Moreover, the individual data sets in the literature only cover a limited temperature range, which prevents deriving reliable physical parameters when applying physical models for the TECs. With the present study, precise data on the thermal expansion of GaN bulk crystals over a wide temperature range of 12 to 1025 K are provided. Because the data can be accurately described by models for the phononic system, reliable values for the characteristic temperatures of GaN are derived as well.

II. EXPERIMENT

The three GaN bulk crystals investigated within this study are unintentionally doped quasi-bulk-like free-standing GaN

(001) layers grown by hydride vapor phase epitaxy (HVPE) and subsequently separated from their substrates by a laser lift-off process. Their thicknesses were 60 μm (sample A), 250 μm (sample B), and 326 μm (sample C), respectively. Whereas samples A and B were fabricated by ourselves, sample C was provided by ATMI (now Cree, Inc.). The HVPE growth was performed on GaN templates fabricated by conventional metalorganic vapor phase epitaxy (MOVPE) for sample A and lateral epitaxial overgrowth by MOVPE for sample B. To our best knowledge sample C was grown without buffer layer directly on sapphire. On the Ga-face of the samples, which was chosen for the measurements, the dislocation density was in the order of $5 \times 10^8 \text{ cm}^{-2}$ (sample A), $3 \times 10^7 \text{ cm}^{-2}$ (sample B), and $1 \times 10^7 \text{ cm}^{-2}$ (sample C), respectively. The room-temperature free electron concentration of samples A and B was below $1 \times 10^{17} \text{ cm}^{-3}$. The resistivity at room temperature for sample C was 0.041 $\Omega \text{ cm}$. The data on samples A, B, and C are combined with our previous data¹⁰ on an unintentionally doped GaN bulk crystal (sample D) grown by a high-pressure (~ 15 kbar) high-temperature (~ 1800 K) method.¹¹ The latter sample had a dislocation density and a room-temperature free electron concentration of below 10^5 cm^{-2} (Ref. 12) and $2 \times 10^{19} \text{ cm}^{-3}$, respectively.¹⁰

Temperature-dependent x-ray measurements were performed with a high-resolution diffractometer (Philips, X-Pert MRD) equipped with a twofold hybrid or a fourfold Ge(220) monochromator and a threefold Ge(220) analyzer. Samples A, B, and C were studied at temperatures in the range from 300 up to 1025 K using an Anton Paar HTK 1200 High Temperature Camera System. The temperature was calibrated with an estimated accuracy of about ± 2 K by measuring single crystalline silicon whose lattice parameters are available for various temperatures.¹³ The GaN lattice parameters c and a were determined by directly measuring the scattering angles with the analyzer crystal¹⁴ for a set of reflections under symmetrical [(002), (004), (006)] and asymmetrical [(214), ($\bar{2}$ 14), (205)] diffraction geometry. For all samples, reciprocal space maps and triple-axis ω scans of (00 l) reflections revealed the existence of several crystalline domains slightly tilted against each other. Precautions were taken to ensure that the same domains were analyzed throughout the temperature-dependent measurements.

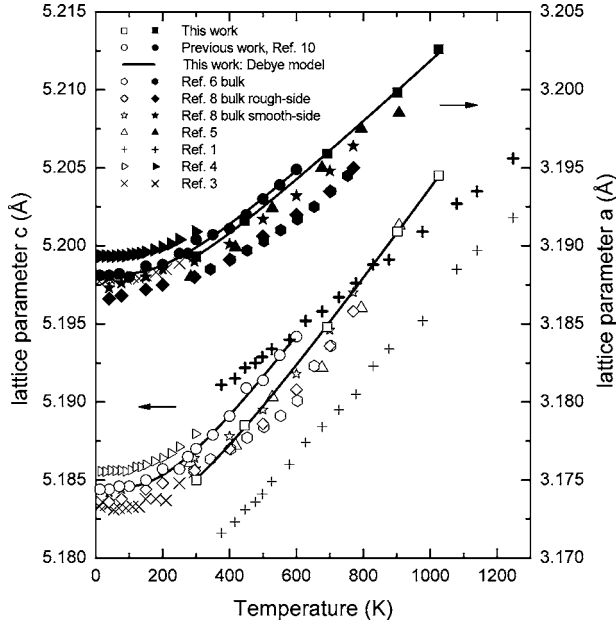


FIG. 1. Temperature dependence of the lattice parameters c (open symbols) and a (filled symbols), of samples C (squares) and D (circles) in comparison with literature data. The solid lines are fits of the Debye model as described in the text.

Sample D was analyzed in the temperature range from 12 up to 600 K using a continuous flow x-ray cryostat from Oxford Instruments. None of the samples showed noticeable hysteresis effects during the temperature cycling.

III. RESULTS AND DISCUSSION

A. Lattice parameters and thermal expansion coefficients

For each temperature the lattice parameters c and a of samples A, B, and C differ by less than 1×10^{-4} Å (c) and 4×10^{-4} Å (a), respectively, which is similar to the accuracy of the experimental setup. Therefore, only the data of sample C and D is presented in Fig. 1 that shows the temperature dependence of the c and a lattice parameters together with literature data. We note that for our data the size of the symbols corresponds to the experimental accuracy of the lattice parameters for a , and it is even larger for c . In the temperature range of 300 to 600 K, where the temperature ranges studied for samples C and D overlap, a constant shift of both lattice parameters c and a of sample D to higher values with respect to sample C is found. This is attributed to a variation of the residual hydrostatic stress in the samples as a result of different impurity levels. An almost linear increase of both lattice parameters c and a can be seen beyond room temperature for samples C and D. In contrast, a decrease of the slope is found for sample D when the latter was cooled below room temperature. Below 100 K there is only a slight change of the lattice parameters c and a with temperature. Figure 1 shows also the literature data mainly on GaN bulk and powder samples taken from Maruska and Tietjen,⁵ Ejder,¹ Paszkowicz *et al.*,³ Leszczynski and co-workers^{6,8} and Reeber

and Wang.⁴ The large scatter of the absolute values of the lattice parameters is again attributed to variations of the residual stress in the investigated samples. It should be emphasized that in comparison to most of the literature data our data reveal a smoother temperature dependence, which we attribute to the superior crystalline perfection of the samples under investigation as well as the high accuracy of our measurements.

To model the experimental data shown in Fig. 1 we follow the approach of treating the anharmonicity of the interatomic potential with a term proportional to the third power of the interatomic spacing.¹⁵ This results in a lattice parameter whose temperature dependence is basically given by the intrinsic energy of the lattice. The latter can be treated within the Debye model or the Einstein model, which are approximations for the acoustic and optical phonons, respectively. Thus, the temperature dependencies of the lattice parameter c can be described by

$$c(T) = c_{0,D} + c_{1,D} \Theta_{D,c} f_D(\Theta_{D,c}/T) \quad (1)$$

and

$$c(T) = c_{0,E} + c_{1,E} \Theta_{E,c} f_E(\Theta_{E,c}/T), \quad (2)$$

respectively. $c_{0,D}$ and $c_{0,E}$ are the lattice parameters at 0 K. $c_{1,D}$ and $c_{1,E}$ are prefactors. $\Theta_{D,c}$ and $\Theta_{E,c}$ are the Debye temperature and the Einstein temperature, respectively, corresponding to the c axis. f_D and f_E are the Debye function and the Einstein function given by

$$f_D(x) = 3 \int_0^1 \frac{t^3}{\exp(tx) - 1} dt \quad (3)$$

and

$$f_E(x) = \frac{1}{\exp(x) - 1}, \quad (4)$$

respectively. In the high-temperature limit, Eqs. (1) and (2) are linear in T with a slope of $c_{1,D}$ and $c_{1,E}$, respectively. The Debye model is supposed to be more accurate than the Einstein model in the low-temperature range where optical phonons are not thermally excited. On the other hand, both models are approximations for the high-temperature range. Here, the complicated dispersion relation of the phonons will be reduced to either a linear slope (Debye model) or a constant (Einstein model).

Both models have been applied to the data shown in Fig. 1. Samples A, B, and C were fitted together with sample D in a single fit routine allowing for a constant offset between the high-temperature data of samples A, B, and C, on the one hand, and the low-temperature data of sample D, on the other. For comparison reasons, samples A, B, and C, on the one hand, and sample D, on the other, were fitted separately by taking the Debye temperature and the Einstein temperature, respectively, from the fit of sample D and keeping it fixed for the fit of the other samples. It was found that the high-temperature slopes $c_{1,D}$ and $c_{1,E}$ differ by less than $\pm 2\%$ whereas the temperatures $\Theta_{D,c}$ and $\Theta_{E,c}$ differ by less than $\pm 3\%$ for the two fit approaches, which is in the order of the statistical accuracy of each individual fit. The implication

TABLE I. Fit parameters and corresponding standard deviations for the temperature dependence of the lattice parameters, c and a , using the Debye model and the Einstein model.

Debye model		Einstein model	
$c_{1,D}$ (10^{-6} Å K $^{-1}$)	29.7 ± 2.3	$c_{1,E}$ (10^{-6} Å K $^{-1}$)	29.6 ± 2.2
$\Theta_{D,c}$ (K)	898 ± 24	$\Theta_{E,c}$ (K)	662 ± 18
$a_{1,D}$ (10^{-6} Å K $^{-1}$)	19.9 ± 1.3	$a_{1,E}$ (10^{-6} Å K $^{-1}$)	19.8 ± 1.1
$\Theta_{D,a}$ (K)	868 ± 20	$\Theta_{E,a}$ (K)	636 ± 13

that the thermal expansion of all samples under study is similar allows us to provide a single data set for the TEC along both a and c direction for the full temperature range.

Figure 1 shows the fit curves for the Debye model as solid lines, which perfectly reproduce the experimental data. This is also true for the Einstein model, the fit curves of which are not shown, however, as they could hardly be distinguished from the curve of the Debye model. The fit parameters for all samples were averaged and are presented in Table I with their corresponding standard deviations. The fitted values for the lattice parameters c_0 at 0 K are 5.1827 Å for sample C and 5.1845 Å for sample D. For the lattice parameters a_0 we obtained 3.1876 and 3.1882 Å, respectively. The TECs which correspond to the first derivatives of Eqs. (1) and (2) divided by the lattice parameter at that temperature are plotted for the fit by the Debye model and the Einstein model in Fig. 2. The fit curves correspond to the average parameter set of all four samples under study as shown in Table I. For comparison, data taken from the literature are shown as well.

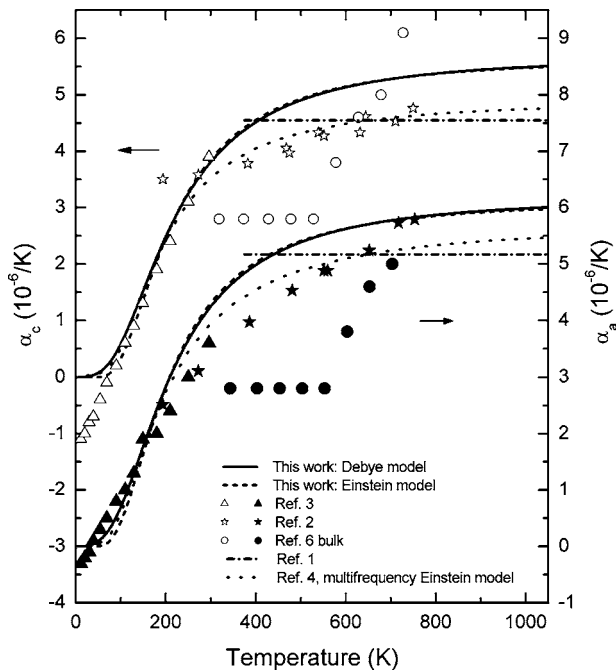


FIG. 2. TECs along c (open symbols) and a (filled symbols) directions of GaN as determined from the fit of the Debye model and the Einstein model in comparison to literature data. The constant TECs proposed by Ejder (Ref. 1) are shown as horizontal lines extending over the measured temperature range.

The data of Sheleg and Savastenko² and Leszczynski *et al.*⁶ are not further considered because of their scatter and unphysical slope, respectively. The data of Maruska and Tietjen⁵ who suggest $\alpha_c = 3.17 \cdots 7.75 \times 10^{-6}$ K $^{-1}$ and $\alpha_a = 5.59 \times 10^{-6}$ K $^{-1}$ in the temperature range from 300 to 900 K are omitted as they scatter significantly. It is noted that the curve for the work of Reeber and Wang⁴ corresponds to a multifrequency Einstein fit to lattice parameters measured by these authors at low temperatures and by Ejder¹ at higher temperatures. Unlike this analytical approach the Debye and Einstein functions used in this work are comparatively simple and still provide an excellent fit of the data. Since Reeber and Wang⁴ did not present their fit together with the experimental data it is difficult to judge on the accuracy of their approach. For temperatures up to 200 K our curves fall close to those presented by Reeber and Wang.⁴ The negative values proposed by Paszkowicz *et al.*³ particularly for α_c at very low temperatures could not be confirmed by our measurements. Considering the scatter of the data in Ref. 3 a negative sign of the TECs at low temperatures seems questionable. A good agreement of our data and that of Paszkowicz *et al.*³ is found in the temperature range of 100 to 300 K. Above room temperature our data indicate TECs that are larger than most values reported by others. In the limit of very high temperatures we obtain $\alpha_c = (5.7 \pm 0.5) \times 10^{-6}$ K $^{-1}$ and $\alpha_a = (6.2 \pm 0.4) \times 10^{-6}$ K $^{-1}$. This compares to $\alpha_c = 4.9 \times 10^{-6}$ K $^{-1}$ and $\alpha_a = 5.7 \times 10^{-6}$ K $^{-1}$ proposed by Reeber and Wang.⁴ The latter values are based on old data of Ejder¹ who by himself, however, reported $\alpha_c = 4.55 \times 10^{-6}$ K $^{-1}$ and $\alpha_a = 5.17 \times 10^{-6}$ K $^{-1}$. Considering the accuracy of both the measurements and the fits along with the extended temperature range under study it is suggested to use our data presented in Fig. 2 as standard values for the TECs of GaN.

B. Debye temperature

Table II gives an overview on the Debye temperatures and Einstein temperatures of GaN reported in the literature. Although the values scatter significantly, it is still found that temperatures derived in this work are mostly larger than those found by others. It should be noted that the experimental values of Refs. 4, 19, 20, and 24 which were derived from measurements that cover an extended temperature range come closest to our values. This could be taken as an indication that the Debye temperature approximates the total phonon spectrum when derived from data covering low and high temperatures whereas it describes the acoustical phonons only when the data are restricted to low temperatures. However, it should be noticed that the Debye model is an approximation even at low temperature as there are longitudinal (LA) and transversal (TA) acoustical phonons with different Debye temperatures. The various measurement techniques collected in Table II average over the acoustical phonons but most likely weigh the TA and LA phonons, respectively, the corresponding elastic constants of the lattice differently. Therefore, care must be taken before using any of the Debye temperatures in Table II including our values as a reference for the dispersion of the acoustical phonons in GaN.

TABLE II. Values reported in the literature for the Debye temperature and the Einstein temperature of GaN, respectively. Lattice parameters (Ref. 4), structural factors (Ref. 16), the Debye-Waller factor (Ref. 17), the refractive index (Ref. 18), the band-gap (Refs. 19 and 20), the phonon density of states (Refs. 21 and 22), the thermal conductivity (Ref. 23), the heat capacity (Refs. 24 and 25), or theory (Refs. 26–28) were used to derive these values.

Ref.	T (K)	Θ_D (K)	Θ_E (K)
Present ($\parallel c$)	12–1025	898 ± 24	662 ± 18
Present ($\parallel a$)	12–1025	868 ± 20	636 ± 13
4 ($\parallel c$)	15–1253		591 ^a
4 ($\parallel a$)	15–1253		581 ^a
16	291	586	
17	10–290		318 ± 25
18	77–300	600	
19	110–630		692 ± 61
20	2–1067	749 ^b	556 ^b
21	8	$\sim 570^c$	
22		560	
23	4.2–300	400 ± 60	
24	5–1073	654	480
25	1.9–10	278 ^d	
26 and 27		600	
28		674	

^aEinstein temperatures of the dominant term in a multifrequency Einstein model fit.

^bThese values were derived by fitting the Debye model and the Einstein model to the fit curve presented in the paper.

^cA temperature dependent Debye temperature was derived which varies between 500 and 870 K.

^dThe small Debye temperature results from values of the heat capacity which are significantly smaller than those reported by others in the literature.

A theoretical estimation of the Debye temperature can be obtained using the elastic properties of the lattice. In general, the velocities of sound v_i for the different phonons propagating in a certain direction ($i=1,2,3$ for one LA and two TA phonons) are calculated by

$$v_i = (A_i/\rho)^{1/2}, \quad (5)$$

where ρ is the density and the coefficients A_i result from the stiffness constants as described in Ref. 29. The average velocity of sound, v , in a certain direction results from averaging the individual velocities of sound v_i corresponding to their contribution to the average phonon density of states, i.e.,

$$v^{-3} = \sum_i v_i^{-3}/3. \quad (6)$$

Then the average Debye temperature in the corresponding direction is given by

$$\Theta_D = \frac{\hbar v}{k_B} \left(\frac{6\pi^2}{\Omega} \right)^{1/3}, \quad (7)$$

where k_B is Boltzmann's constant and Ω is the volume of the unit cell.³⁰ The results from Eq. (7) can be found in the columns 2 and 3 of Table III for various sets of stiffness constants reported in the literature. Averaging these values by omitting Refs. 31 and 36 suggests Debye temperatures of $\Theta_{D,c}=590$ K and $\Theta_{D,a}=610$ K. These values come close to most of the values listed in Table II for experiments performed at or below room temperature and all the values suggested by theory. However, there are other values including ours that are considerably larger. In addition, the columns 4 and 5 of Table III show values for the Debye temperatures if only LA phonons are taken into account. The higher sound velocity of the LA phonons in comparison to the TA phonons leads to significantly higher characteristic temperatures with

TABLE III. Values for the Debye temperatures derived from the stiffness constants reported in the literature. The sound velocity was calculated by considering the phonon propagation ($\Theta_{D,c}, \Theta_{D,a}$) and the hydrostatic pressure (Θ_D), respectively.

Refs.	Phonon propagation				Hydrostatic pressure Θ_D (K)	$\sqrt{c_{33}/c_{11}}$
	TA and LA phonons		LA phonons			
	$\Theta_{D,c}$ (K)	$\Theta_{D,a}$ (K)	$\Theta_{D,c}$ (K)	$\Theta_{D,a}$ (K)		
31	300	359	875	922	747	0.950
32	615	636	1069	1058	776	1.010
33	625	631	1046	1024	765	1.022
34	528	556	1078	997	760	1.082
35	587	611	1078	1026	762	1.050
36	533	578	775	1040	704	0.745
37	603	607	1039	1002	752	1.036
38	571	599	1058	1031	770	1.027
39	562	576	964	951	708	1.014
40	583	610	1054	1035	743	1.019
41	582	609	1054	1035	743	1.019
42	649	669	1067	1029	712	1.037

average values of $\Theta_{D,c}=1051$ K and $\Theta_{D,a}=1019$ K. Since these numbers are beyond the values determined in this study, the thermal expansion of the lattice should be stronger governed by the LA phonons than by the TA phonons. The same conclusion can be drawn when using the bulk modulus as given in Ref. 43 for the coefficients A_i in Eq. (5). This approach results from the analogy between the thermal expansion and a hydrostatic pressure as in both cases the lattice expands in all directions simultaneously. The respective Debye temperatures are shown in column 6 of Table III. Again they are significantly larger than the values derived from averaging the LA and TA phonon propagation which suggests that the Debye temperatures of the thermal expansion are underestimated when they are calculated using the average sound velocity in the corresponding direction.

It should be noted that our experimentally determined Debye temperature in the c direction is larger than that in the a direction which can be attributed to the elastic anisotropy of the wurzite lattice of GaN. The stiffness constants which are relevant for the normal stresses in these directions are c_{33} and c_{11} . Since the Debye temperature is proportional to the square root of the stiffness constants as can be seen in Eq. (5), the square root ratio of c_{33} and c_{11} is listed in the last column of Table III. Using the Debye temperatures derived

in this study (compare Table II) $\Theta_{D,c}/\Theta_{D,a}=1.035\pm 0.051$. This fits nicely to most values given in Table III.

IV. SUMMARY

Temperature-dependent high-resolution x-ray diffraction measurements were used to derive precise thermal expansion coefficients for bulk GaN over an extended temperature range between 12 and 1025 K. The provided data can serve as reference values for the thermal expansion of GaN. The Debye and Einstein models were found to be capable of describing the data accurately. In comparison to experimental values reported in the literature our determined Debye and Einstein temperatures are similar in some cases but higher in others. A theoretical estimation of the Debye temperature from the elastic stiffness constants suggests that the various experimental techniques weigh the TA and LA phonons, respectively, the corresponding elastic constants of the lattice differently.

ACKNOWLEDGMENTS

The authors thank Tanya Paskova and Bo Monemar at Linköping University for the growth of the samples. This work was supported by the Deutsche Forschungsgemeinschaft under Contracts No. HE 2827/5-1 and HO 1388/25-2.

*Electronic address: croder@ifp.uni-bremen.de

- ¹E. Ejder, Phys. Status Solidi A **23**, K87 (1974).
- ²A. U. Sheleg and V. A. Savastenko, Vestsi Akad. Navuk BSSR, Ser. Fiz.-Mat. Navuk **3**, 126 (1976).
- ³W. Paszkowicz, J. Z. Domagala, J. A. Sokolowski, G. Kamler, S. Podsiadlo, and M. Knapp, in *Synchrotron Radiation Studies of Materials: Proceedings of 5th National Symposium of Synchrotron Radiation Users*, edited by M. Lefeld-Sosnowska and J. Gronkowski (Zaklad Graficzny Uniwersytetu Warszawskiego, Warsaw, 1999), pp. 183–189.
- ⁴R. R. Reeber and K. Wang, J. Mater. Res. **15**, 40 (2000).
- ⁵H. P. Maruska and J. J. Tietjen, Appl. Phys. Lett. **15**, 327 (1969).
- ⁶M. Leszczynski, T. Suski, H. Teisseyre, P. Perlin, I. Grzegory, J. Jun, S. Porowski, and T. D. Moustakas, J. Appl. Phys. **76**, 4909 (1994).
- ⁷M. Leszczynski, T. Suski, P. Perlin, H. Teisseyre, I. Grzegory, M. Bockowski, J. Jun, S. Porowski, and J. Major, J. Phys. D **28**, A149 (1995).
- ⁸M. Leszczynski, H. Teisseyre, T. Suski, I. Grzegory, M. Bockowski, J. Jun, B. Palosz, S. Porowski, K. Pakula, J. M. Baranowski, and A. Barski, Acta Phys. Pol. A **90**, 887 (1996).
- ⁹H. Heinke, V. Kirchner, S. Einfeldt, U. Birkle, and D. Hommel, J. Cryst. Growth **189/190**, 375 (1998).
- ¹⁰V. Kirchner, H. Heinke, D. Hommel, J. Z. Domagala, and M. Leszczynski, Appl. Phys. Lett. **77**, 1434 (2000).
- ¹¹S. Porowski, J. Cryst. Growth **189/190**, 153 (1998).
- ¹²M. Leszczynski, I. Grzegory, M. Bockowski, J. Jun, S. Porowski, J. Jasinski, and J. M. Baranowski, Acta Phys. Pol. A **88**, 799 (1995).
- ¹³H. Ibach, Phys. Status Solidi **31**, 625 (1969).
- ¹⁴P. F. Fewster and N. L. Andrew, J. Appl. Crystallogr. **28**, 451 (1995).
- ¹⁵Ch. Weißmantel and C. Hamann, *Grundlagen der Festkörperphysik* (Springer, Heidelberg, 1995), p. 317.
- ¹⁶X. L. Chen, J. K. Liang, Y. P. Xu, T. Xu, P. Z. Jiang, Y. D. Yu, and K. Q. Lu, Mod. Phys. Lett. B **13**, 285 (1999).
- ¹⁷M. Katsikini, H. Rossner, M. Fieber-Erdmann, E. Holub-Krappe, T. D. Moustakas, and E. C. Paloura, J. Synchrotron Radiat. **6**, 561 (1999).
- ¹⁸E. Ejder, Phys. Status Solidi A **6**, 445 (1971).
- ¹⁹J. Petalas, S. Logothetidis, S. Boultradakis, M. Alouani, and J. M. Wills, Phys. Rev. B **52**, 8082 (1995).
- ²⁰R. Pässler, Phys. Status Solidi B **216**, 975 (1999).
- ²¹J. C. Nipko, C.-K. Loong, C. M. Balkas, and R. F. Davis, Appl. Phys. Lett. **73**, 34 (1998).
- ²²C.-K. Loong, J. Eur. Ceram. Soc. **19**, 2241 (1999).
- ²³A. Jezowski, B. A. Danilchenko, B. Boćkowski, I. Grzegory, S. Krukowski, T. Suski, and T. Paszkiewicz, Solid State Commun. **128**, 69 (2003).
- ²⁴J. Unland, B. Onderka, A. Davydov, and R. Schmid-Fetzer, J. Cryst. Growth **256**, 33 (2003).
- ²⁵Y. T. Song, X. Wu, W. J. Wang, W. X. Yuan, and X. L. Chen, J. Alloys Compd. **370**, 65 (2004).
- ²⁶E. F. Steigmeier, Appl. Phys. Lett. **3**, 6 (1963).
- ²⁷G. A. Slack, J. Phys. Chem. Solids **34**, 321 (1973).
- ²⁸S. Yu. Davydov and S. K. Tikhonov, Semiconductors **30**, 514 (1996).
- ²⁹R. Truell, C. Elbaum, and B. Chick, *Ultrasonic Methods in Solid State Physics* (Academic Press, New York, 1969), p. 15.
- ³⁰Ch. Weißmantel and C. Hamann, *Grundlagen der Festkörper-*

- physik* (Springer, Heidelberg, 1995), p. 302.
- ³¹V. A. Savastenko and A. U. Sheleg, *Phys. Status Solidi A* **48**, K135 (1978).
- ³²A. Polian, M. Grimsditch, and I. Grzegory, *J. Appl. Phys.* **79**, 3343 (1996).
- ³³M. Yamaguchi, T. Yagi, T. Azuhata, T. Sota, K. Suzuki, S. Chichibu, and S. Nakamura, *J. Phys.: Condens. Matter* **9**, 241 (1997).
- ³⁴K. Kim, W. R. L. Lambrecht, and B. Segall, *Phys. Rev. B* **56**, 7018 (1997).
- ³⁵A. F. Wright, *J. Appl. Phys.* **82**, 2833 (1997).
- ³⁶R. B. Schwarz, K. Khachatryan, and E. R. Weber, *Appl. Phys. Lett.* **70**, 1122 (1997).
- ³⁷K. Shimada, T. Sota, and K. Suzuki, *J. Appl. Phys.* **84**, 4951 (1998).
- ³⁸C. Deger, E. Born, H. Angerer, O. Ambacher, M. Stutzmann, J. Hornsteiner, E. Riha, and G. Fischerauer, *Appl. Phys. Lett.* **72**, 2400 (1998).
- ³⁹V. Yu. Davydov, Yu. E. Kitaev, I. N. Goncharuk, A. N. Smirnov, J. Graul, O. Semchinova, D. Uffmann, M. B. Smirnov, A. P. Mirgorodsky, and R. A. Evarestov, *Phys. Rev. B* **58**, 12899 (1998).
- ⁴⁰M. Yamaguchi, T. Yagi, T. Sota, T. Deguchi, K. Shimada, and S. Nakamura, *J. Appl. Phys.* **85**, 8502 (1999).
- ⁴¹T. Deguchi, D. Ichiryu, K. Toshikawa, K. Sekiguchi, T. Sota, R. Matsuo, T. Azuhata, M. Yamaguchi, T. Yagi, S. Chichibu, and S. Nakamura, *J. Appl. Phys.* **86**, 1860 (1999).
- ⁴²T. Azuhata, T. Sota, and K. Suzuki, *J. Phys.: Condens. Matter* **8**, 3111 (1996).
- ⁴³J. F. Nye, *Physical Properties of Crystals* (Oxford University Press, London, 1969), p. 146.